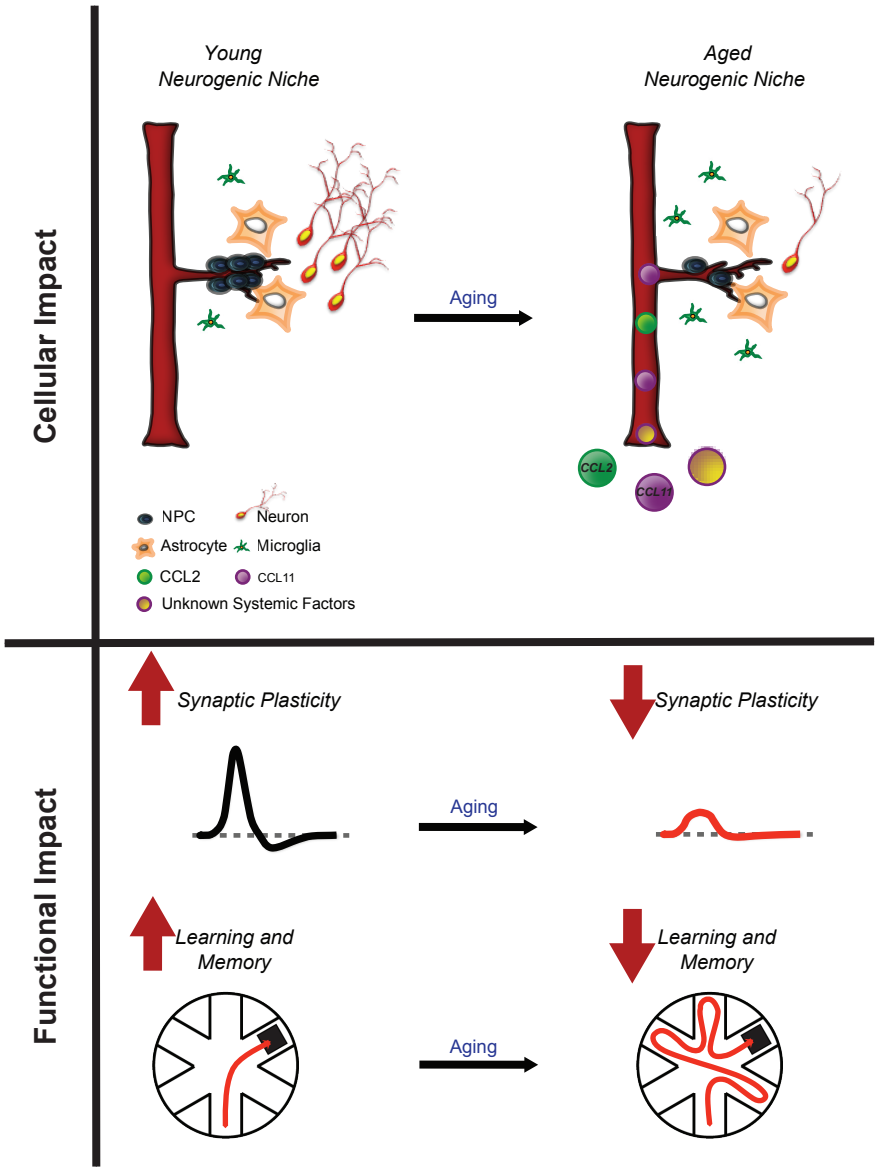

S1. Proposed model illustrating the cellular and functional impact of age-related systemic molecular changes on the adult neurogenic niche. Schematic of cellular changes occurring in the neurogenic niche during normal aging and heterochronic parabiosis. Levels of blood-borne factors, including the chemokines CCL11 and CCL2, increase during normal aging and heterochronic parabiosis. These systemic changes contribute to the decline in neurogenesis observed in the adult brain and functionally impair synaptic plasticity and learning and memory. Cell types illustrated include neural stem cells (blue), neurons (red), astrocytes (orange) and microglia (green).

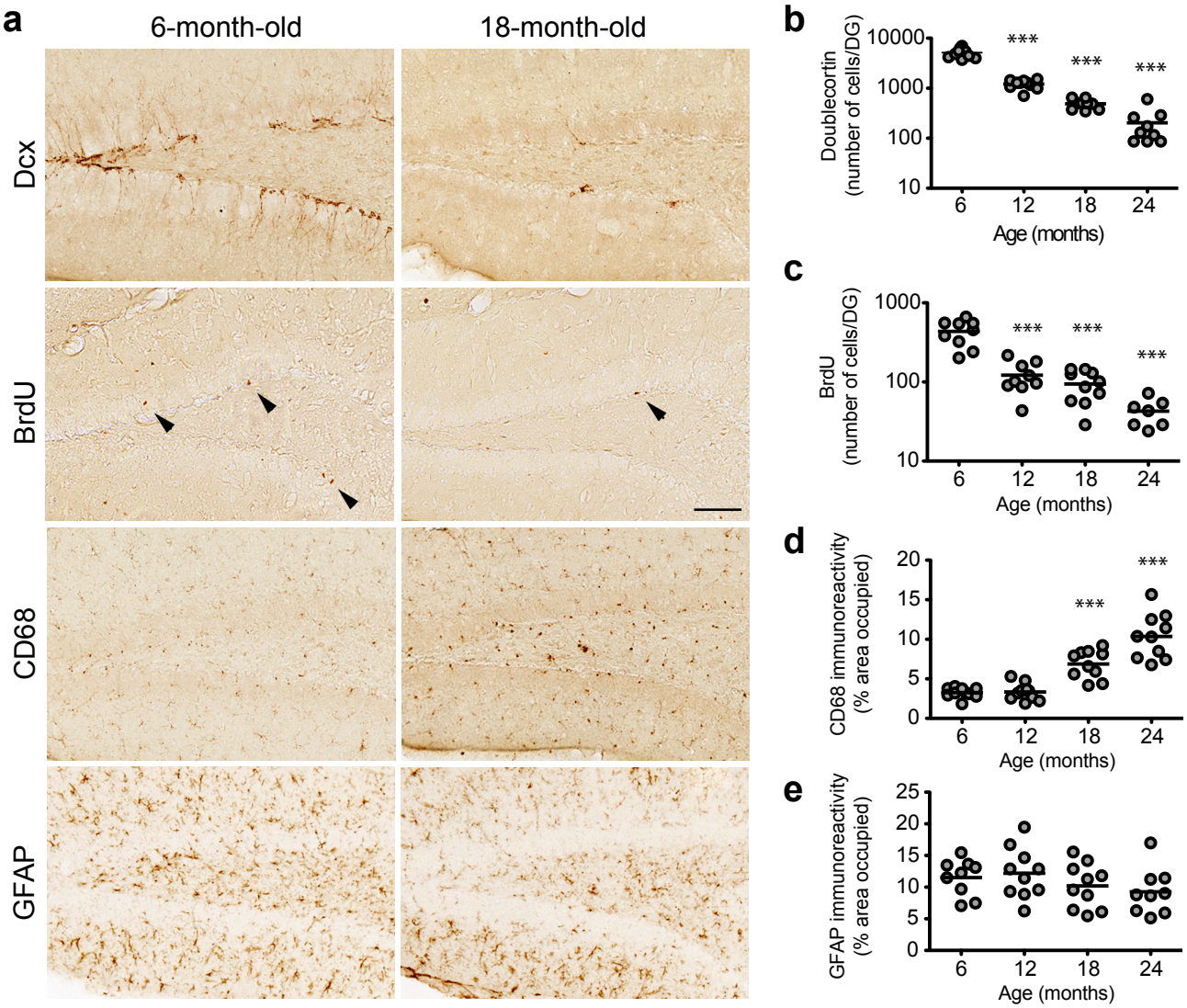

S2. Cellular characterization of the adult dentate gyrus during aging. a, Immunohistochemical detection of of newly differentiated Doublecortin (Dcx)-positive neurons, long-term BrdU-retaining cells (arrowheads), CD68-positive activated microglia, and GFAP-positive astrocytes in the DG of the hippocampus from adult mice at 6 and 18 months of age (scale bar: 100 µm). **b-d,** Quantification of age-related cellular changes in the adult DG. Data are from 5-10 mice per age group, each dot represents the mean number per mouse. **b,** Age-related decrease in neurogenesis. **c,** Animals were given BrdU injections for 6 days and euthanized 21 days following the last injection. **d,** Age-related increase of relative immunoreactivity to CD68, a marker for microglia activation. **e,** GFAP immunoreactivity did not significantly change with age. Dot plots with mean; ***P< 0.001, ANOVA, Dunnet's post-hoc test.

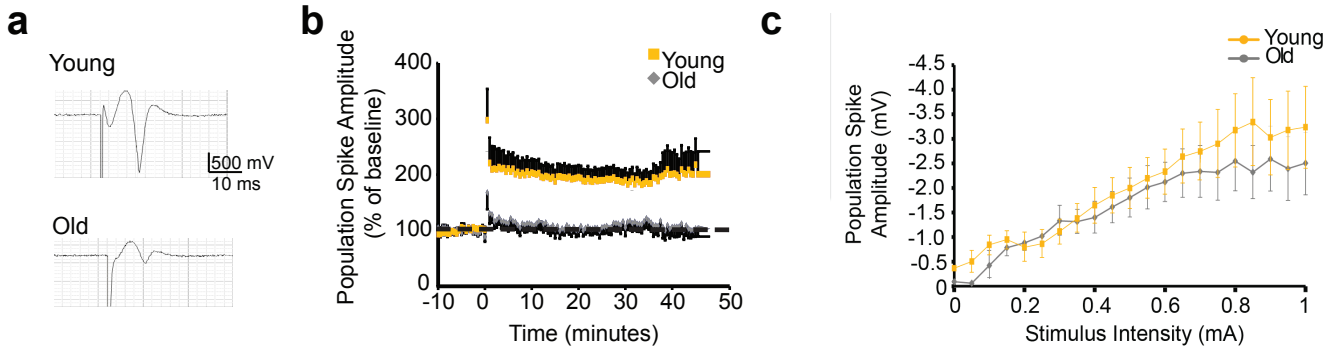

S3. Electrophysiological assessment of the adult dentate gyrus during aging. a,b, Synaptic plasticity of normal aging animals was examined in hippocampal slices by extracellular electrophysiological recordings using a long-term potentiation (LTP) paradigm. **a,** Representative electrophysiological profiles collected from individual young (3 months) and old (18 months) mice during LTP recordings from the DG. **b,** LTP levels recorded from the DG were lower in the hippocampus of old versus young animals following 40 minutes post induction. **c,** input-output curves indicate no statistical difference in synaptic strength, a key parameter of basal synaptic transmission, between young (3 months) and old (18 months) animals although a tendency of synaptic weakening is observed during aging.

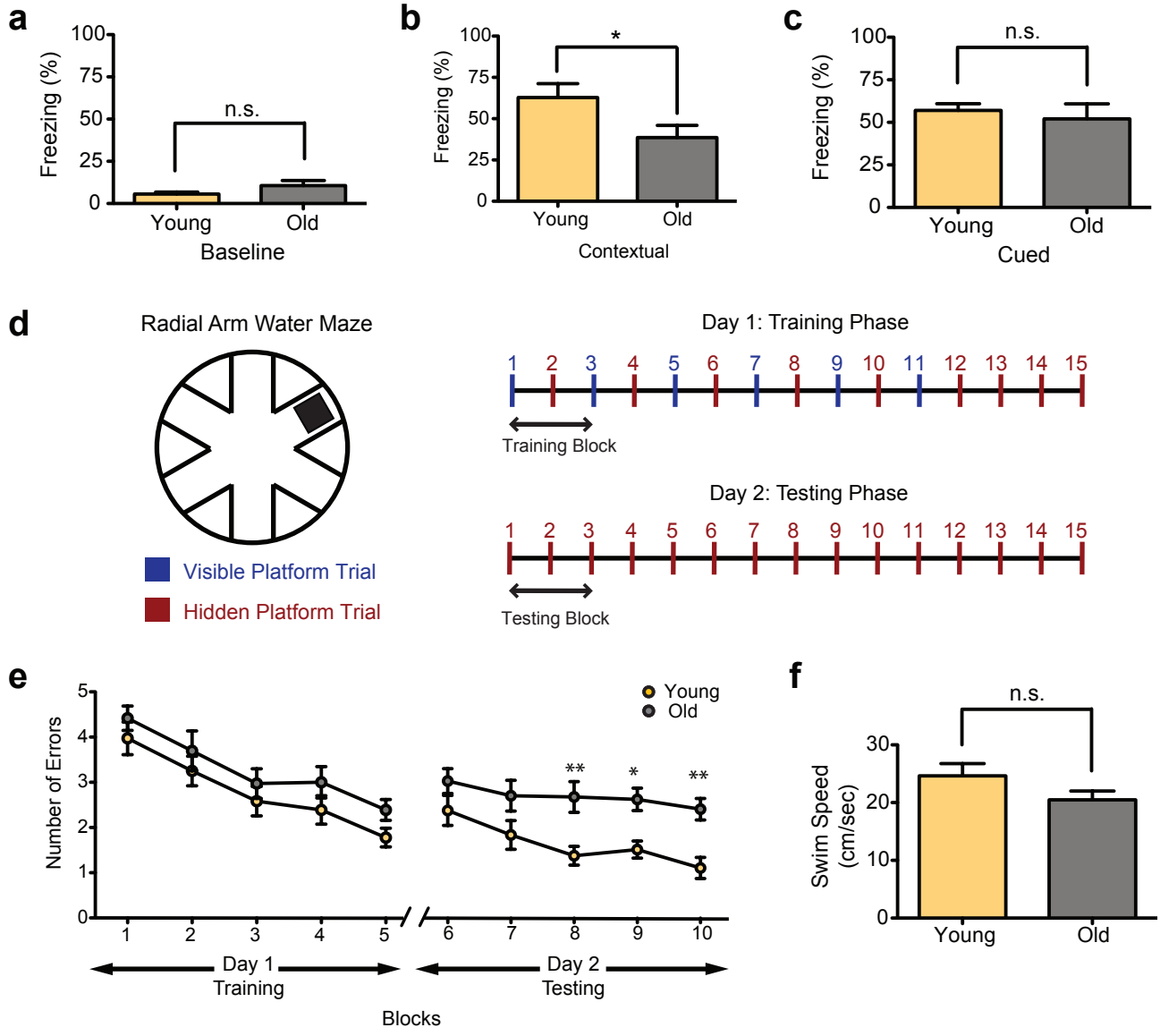

S4. Characterization of cognitive function during aging. a-f, Learning and memory was examined during normal aging in young (2-3 months) versus old (18-20 months) adult animals using contextual fear conditioning **(a-c)** and RAWM **(d-f)** paradigms. **a**, Young and old animals exhibited similar baseline freezing time during fear conditioning training. **b,** During contextual fear conditioning old mice demonstrate decreased freezing time. **c,** No differences in cued memory were detected 24 hours after training when re-exposed to the conditioned stimulus (tone and light) in a novel context. Data are from 8-10 animals per group. **d,** A schematic of the RAWM paradigm. The goal arm location containing the platform remains constant, while the start arm is changed during each trial. On day one during the training phase, mice are trained for 15 trials, with trials alternating between visible (blue) and hidden (red) platform. On day two during the testing phase, mice are tested for 15 trials with the hidden (red) platform. Entry into an incorrect arm is scored as an error, and errors are averaged over training blocks (three consecutive trials). **e,** Old mice demonstrate impaired learning and memory for platform location during the testing phase of the task. Cognitive deficits were quantified as the number of entry arm errors made prior to finding the target platform. **f,** Swim speeds of young and old animals during training. Data are from 12 mice per age group. All data are represented as Mean + SEM; *P< 0.05; **P< 0.01; n.s. not significant; t-test **(a-c,f)**, repeated measures ANOVA, Bonferroni post-hoc test **(e)**.

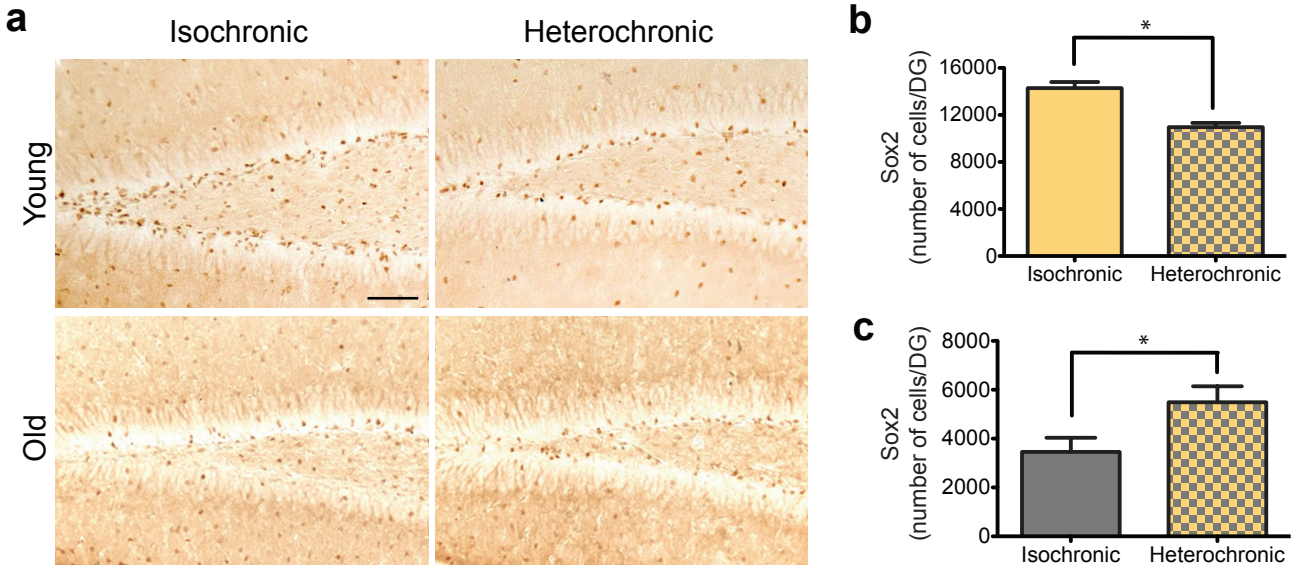

S5. Heterochronic parabiosis reduces progenitor frequency in the DG of young animals while increasing frequency in aged animals. a, A representative field of Sox2 immunostaining is shown for young (3-4 months) and aged (18-20 months) isochronic and heterochronic parabionts five weeks after parabiosis (scale bar: 100 μm). **b,** Quantification of Sox2-positive progenitor cells in the young DG after parabiosis. Data are from 8 mice for isochronic and 6 mice for heterochronic groups. **c,** Quantification of Sox2-positive cells in the aged DG after parabiosis. Data are from 4 mice for isochronic and 6 mice for heterochronic groups. Bars are mean + SEM; *P< 0.05.

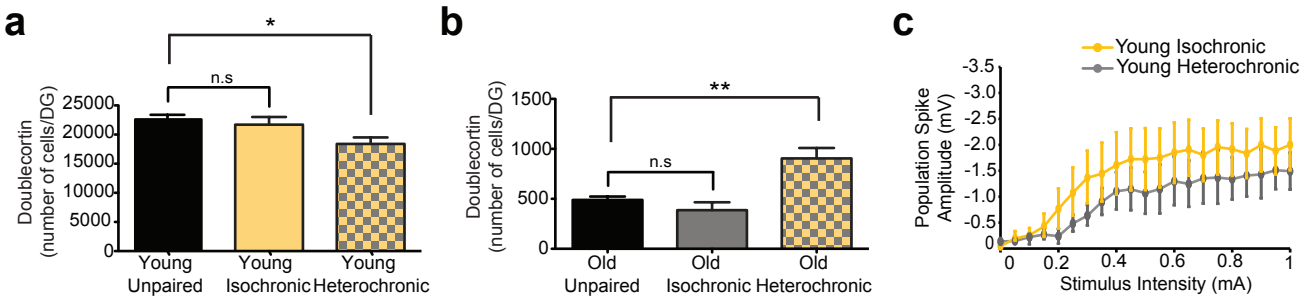

S6. Isochronic parabiosis does not alter neurogenesis or synaptic transmission. a,b, Quantification of neurogenesis (Dcx, Doublecortin-positive cells) in the DG during normal aging and after isochronic or heterochronic parabiosis. Data are from 10 normal young (3 months) mice, 10 young isochronic parabionts (3-4 months) and 12 young heterochronic parabionts (3-4 months), 10 normal aged (18 months) mice, 6 old isochronic parabionts (18-20 months) and 12 old heterochronic parabionts (18-20 months). **c,** input-output curves indicate no statistically significant difference in synaptic transmission strength between young isochronic and young heterochronic parabionts. Bars are mean + SEM; *P< 0.05; **P< 0.01; n.s., not significant; ANOVA, Dunnet's post-hoc test.

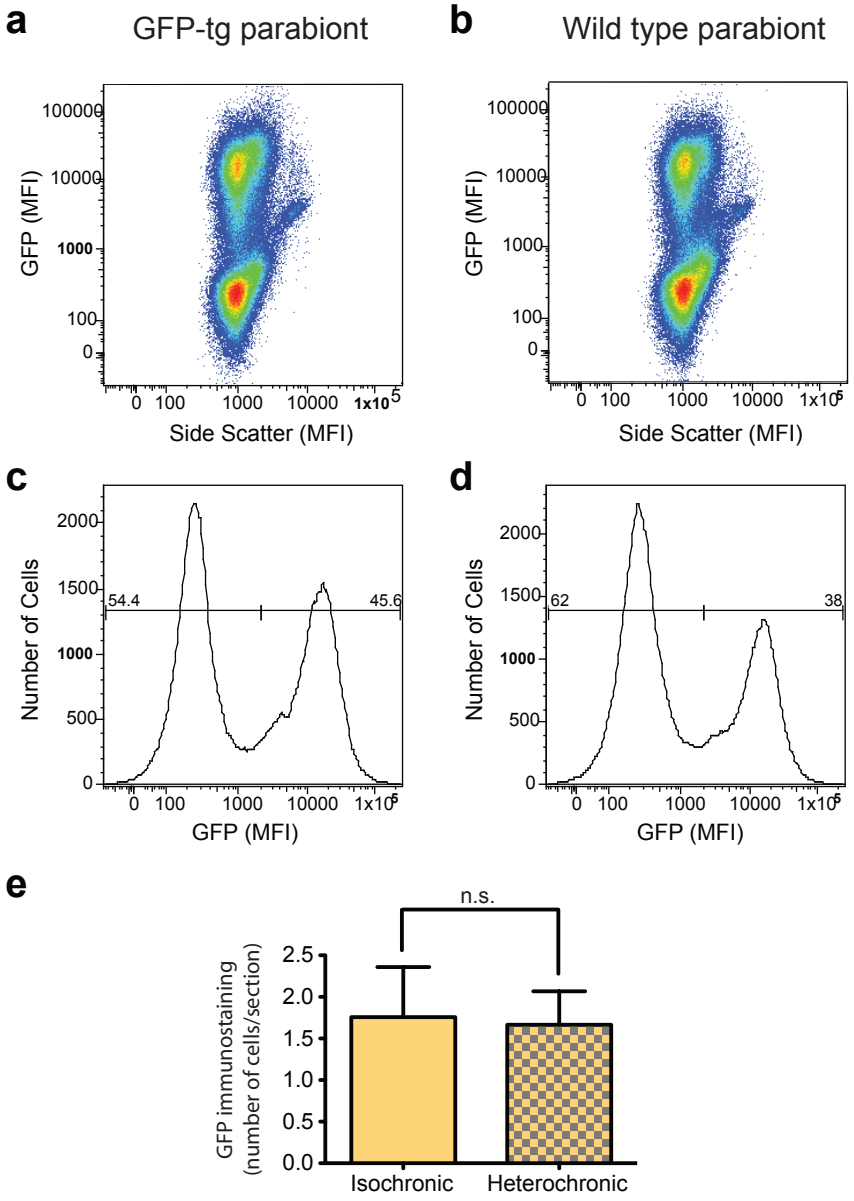

S7. A circulatory system is shared between animals during parabiosis. a-d, A subset of four parabiotic pairs were generated by joining young (2-3 months old) actin-GFP transgenic with young (2-3 months old) and aged (18 months old) non-transgenic mice. Blood was isolated two weeks after surgery and flow cytometric analysis was done on fixed and permeabilized blood cells. Representative flow-cytometry plots demonstrate the frequency of GFP-positive cells in a GFP-transgenic (tg) parabiont (a,c) and wild-type (wt) parabiont (b,d) at the time of sacrifice. MFI, mean fluorescence intensity. **e,** Quantification of GFP-positive cells in the DG of the hippocampus in young and aged wild-type parabionts after parabiosis with young actin-GFP-positive parabionts. 5 sections per mouse; bars are mean + SEM; n.s., not significant; t-test.

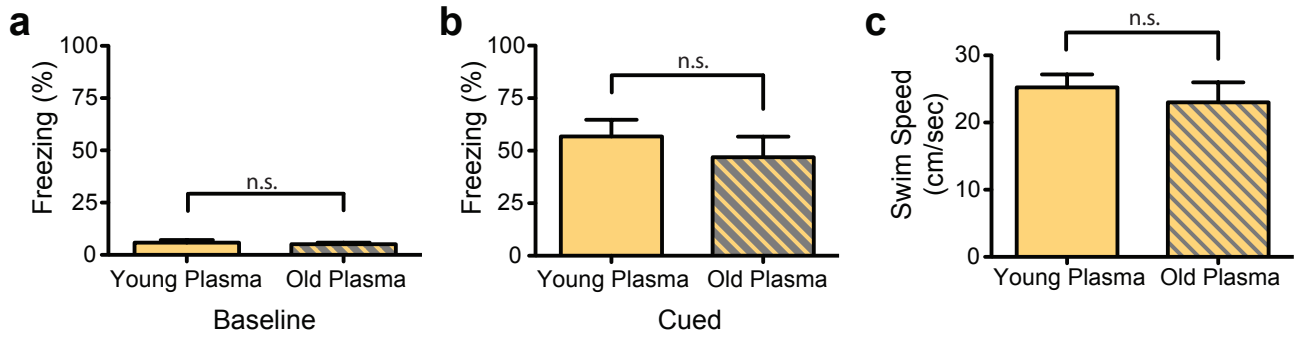

S8. Cued memory and swim speeds are not altered by aged plasma administration. a-c, Young adult male mice (3 months) were injected intravenously with young (3-4 months) or old (18-22 months) plasma nine times over 24 days. **a,b,** Conditioned fear was displayed as freezing behavior. **a,** Animals intravenously injected with young or old plasma exhibited similar baseline freezing time during training. **b,** No differences in cued memory were detected between groups when re-exposed to the conditioned stimulus (tone and light) in a novel context 24 hours after training. Data are from 8 mice per group. **c,** Swim speeds of young or old plasma treated mice during the training phase of the RAWM. Data are from 12 mice per group. Bars are mean + SEM; n.s., not significant; t-test.

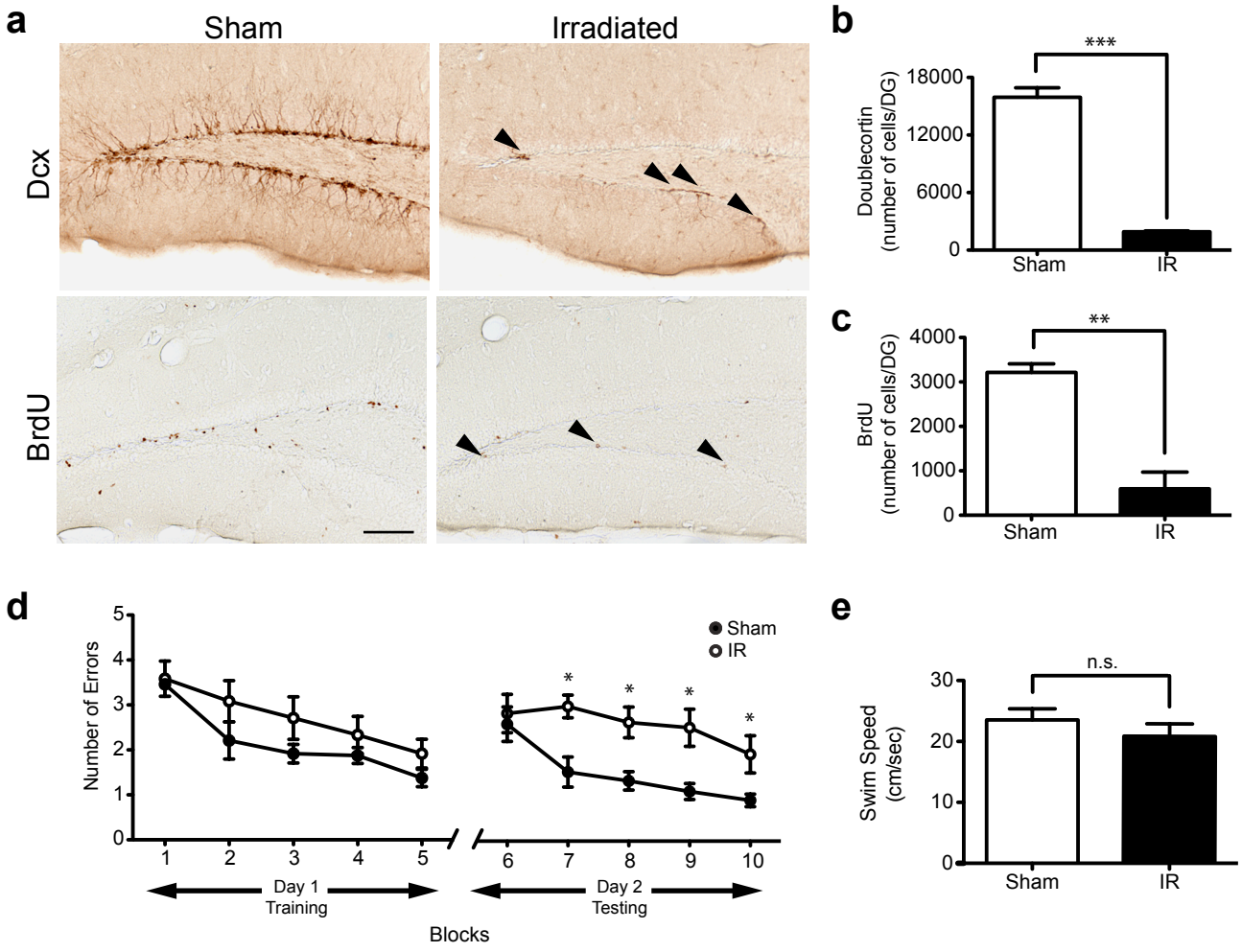

S9. Ablation of hippocampal neurogenesis by irradiation results in impaired learning and memory in the RAWM paradigm. a-e, Young adult male mice (3 months) were irradiated with 5Gy gamma radiation three times over eight days. **a-c,** Neurogenesis and cell proliferation were analyzed by immunostaining for Doublecortin (Dcx) and Bromodeoxyuridine (BrdU) respectively. **a,** A representative field of Dcx-positive and BrdU-positive cells is shown for each treatment group. (scale bar: 100 μm). **b,c** Quantification of neurogenesis (**b**) and proliferation (**c**) in the DG after cranial irradiation. Data are from 8-10 mice per group. **d,e,** Hippocampal learning and memory was assessed using the RAWM paradigm in young (3 months) adult male mice in which neurogenesis was ablated by irradiation. **d,** During the RAWM task learning and memory deficits were quantified as the number of entry arm errors made prior to finding the target platform. **e,** Swim speeds of sham irradiated and irradiated mice during the training phase of the RAWM. Data are from 8 irradiated and 10 control sham mice. All data are represented as Mean + SEM; *P< 0.05; **P< 0.01; ***P< 0.001; t-test (b,c,e), repeated measures ANOVA, Bonferroni post-hoc test (d).

a

Name	Score(d)	q-value(%)
CCL11	-1.40	0
CCL2	-1.39	0
CXCL10	-1.29	0
SGOT	-1.12	0
Haptoglobin	-1.10	0
Osteopontin	-1.09	0
CXCL2	-1.08	0
vWF	-0.99	0
CCL7	-0.98	0
CCL19	-0.92	0
CCL9	-0.89	2.80
TIMP-1	-0.82	2.80
XCL1	-0.82	2.80
β2-Microglobulin	-0.82	2.80
Leptin	-0.67	7.33
CCL12	-0.67	7.33
CCL22	-0.64	7.33

c

Protein Factor	Fold Change (versus Isochronic)	
	Young Heterochronic	Old Heterochronic
CD40	n.c	-1.4 ± 0.1
CCL11	2.1 ± 0.3	n.c
CXCL6	3.5 ± 0.4	n.c
Haptoglobin	8.5 ± 0.6	-1.4 ± 0.1
IL-11	8.5 ± 1.4	4.6 ± 1.5
IL-1α	6.5 ± 1.1	-1.4 ± 0.1
IL-5	2.2 ± 0.2	-1.6 ± 0.04
IL-7	6.5 ± 1.0	n.c
CXCL1	7.3 ± 1.1	n.c
CCL2	2.3 ± 0.2	n.c
CCL12	2.1 ± 0.1	n.c
CCL4	2.9 ± 0.3	n.c
CCL19	2.2 ± 0.1	n.c
Myoglobin	2.9 ± 0.6	n.c
β2-Microglobulin	17.7 ± 1.7	n.c
MPO	2.8 ± 0.3	n.c

b

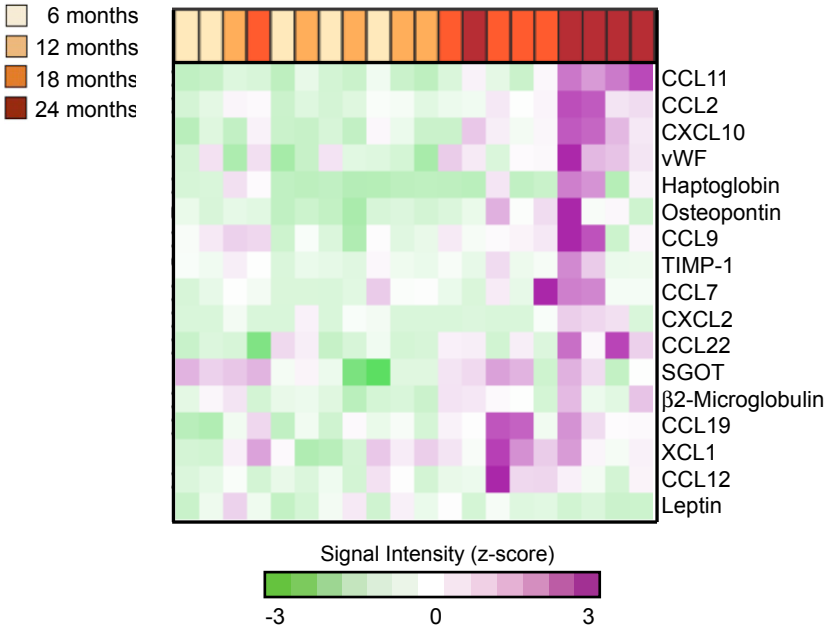

S10. Changes in concentrations of selected secreted plasma proteins correlate with declining neurogenesis in aging and heterochronic parabiosis. a. Analysis of plasma protein correlations with decreased neurogenesis in the aging mouse samples using the Significance Analysis of Microarray software (SAM 3.00 algorithm). SAM assigns d-scores to each gene or protein on the basis of a multi-comparison analysis of expression changes and indicates significance by q-value. **b,** Unsupervised clustering of secreted signaling factors that were significantly associated with age-related decreased neurogenesis with a false discovery rate of 7.34% or less (SAM, q ≤ 7.34). Mouse age groups are indicated at the top of the node map as boxes in which youngest ages are tan and oldest ages are red. Thus cluster analysis of systemic factors associated with decreased neurogenesis also produce a reasonable separation of samples by age. Color shades in the node map indicate higher (purple) or lower (green) relative plasma concentrations. **c,** Quantitative fold changes in soluble signaling factors between isochronic versus heterochronic parabiotic groups. Color shades indicate increases (pink) and decreases (green) in relative plasma concentrations. All data represented as mean ± SEM of fold changes observed with parabiosis; n.c. denotes no significant change.

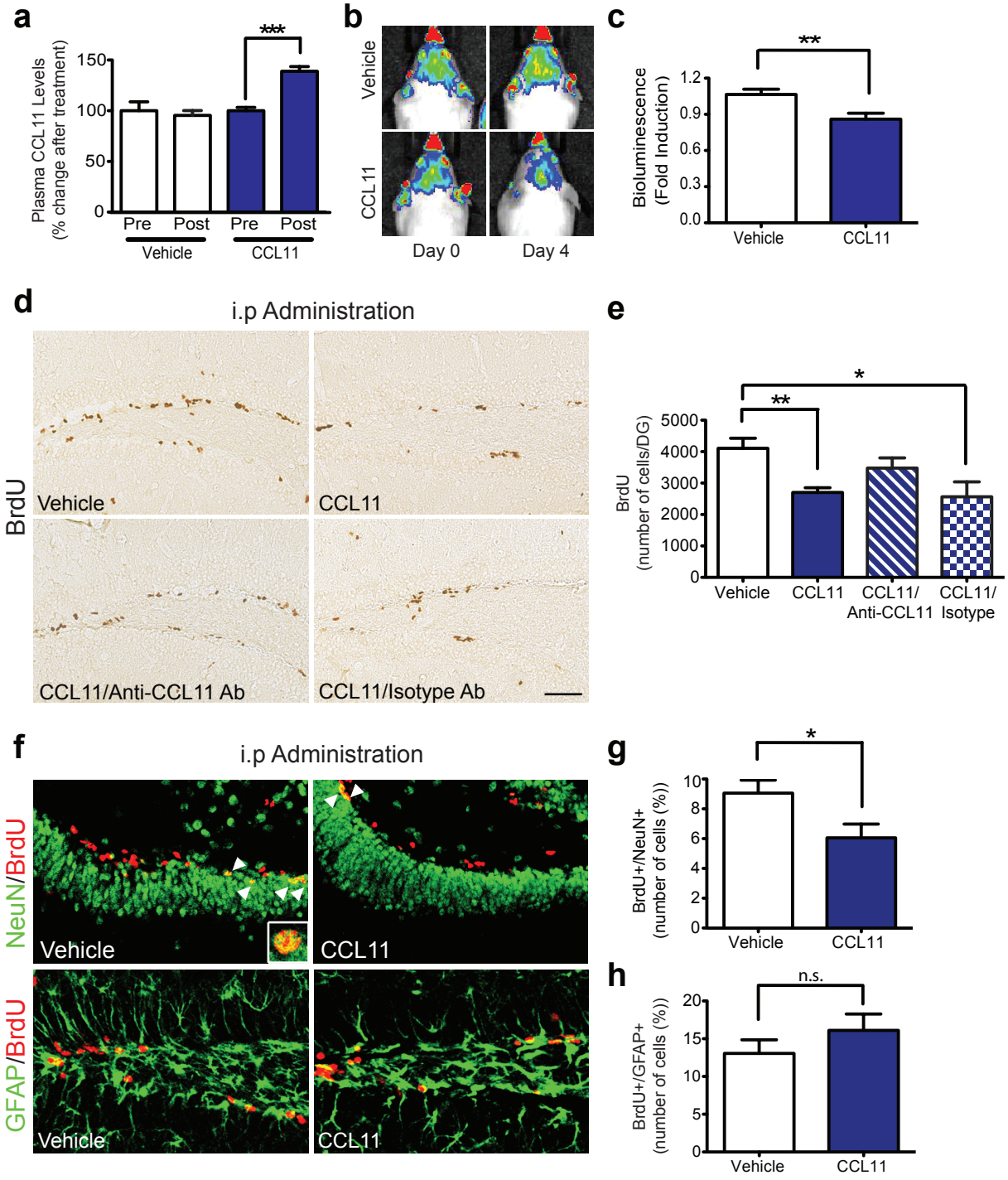

S11. Systemic administration of CCL11 reduces neuronal but not glial differentiation in young animals. a, An increase in CCL11 plasma levels was detected by ELISA in mice treated systemically with CCL11. **b,** Dcx-luc reporter mice (2-3 months) were injected with CCL11 or PBS (vehicle) on days 0, 2, and 4. Representative bioluminescence recording images shown for each treatment group. **c,** Bioluminescence was quantified as photons/s/cm2/steridan and differences expressed as changes in fold-induction between day 0 and 4. Data from 7 mice per group. **d-h,** Young adult mice (2-3 months old) were injected with CCL11 or vehicle through intraperitoneal injections four times over ten days. Animals were injected with BrdU for three days prior to sacrifice. **d,** A representative field of BrdU immunostaining in the DG is shown for each treatment group. (scale bar: 100 µm). **e,** Quantification of BrdU-positive cells in the DG after systemic drug administration. Data are from 5-10 mice per group. **f,** Representative confocal microscopy images DG of brain sections immunostained for BrdU (red) in combination with NeuN (green) or GFAP (green) shown for both treatment groups. Inset depicts a high magnification image of a cell co-labeled with BrdU and NeuN (scale bar: 100 µm). **g,h,** Quantification of the relative number of BrdU and either NeuN (**g**) or GFAP (**h**) double positive cells out of all BrdU-positive cells. Data from 5 mice per group. Bars show mean + SEM; *P< 0.05; **P< 0.01; ***P< 0.001; n.s., not significant; t-test (**c,g,h**) or ANOVA, Dunnet's post-hoc test (**a,e**).

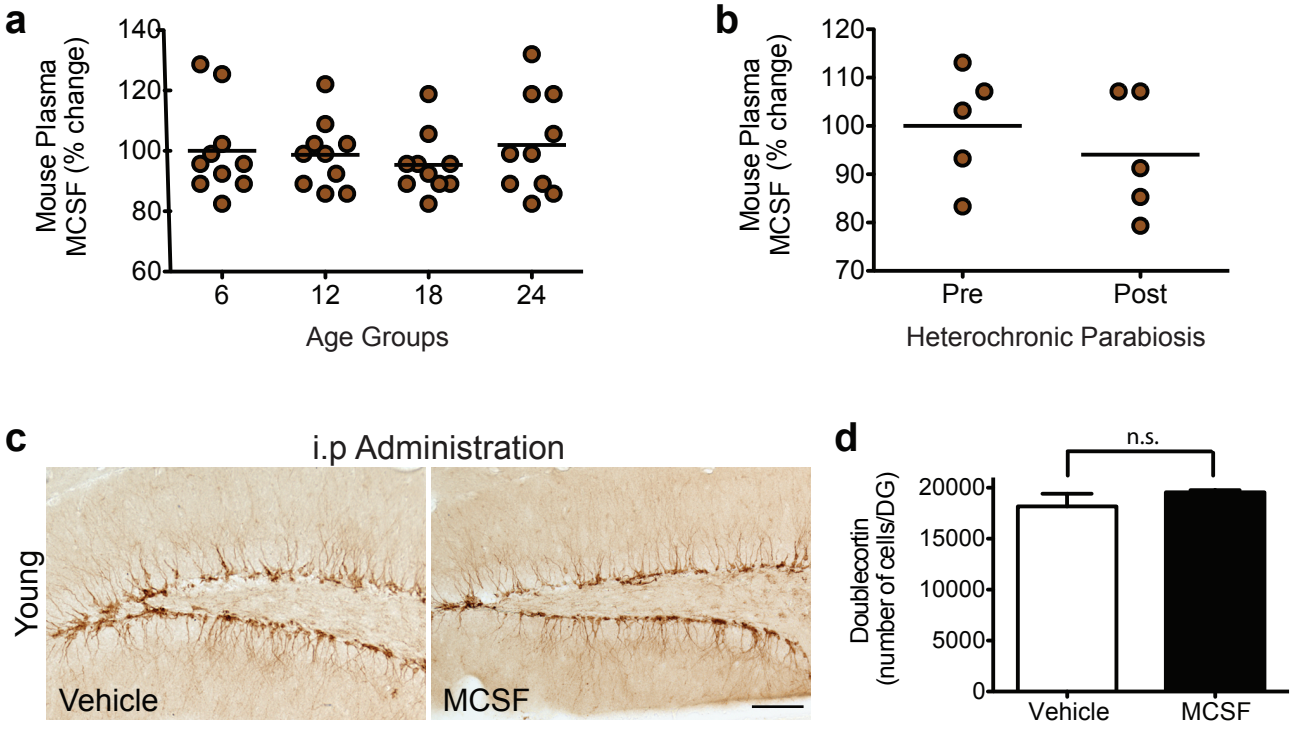

S12. Systemic administration of MCSF does not alter neurogenesis in the DG of young animals. a,b Plasma concentrations for MCSF in normal aged (6, 12, 18 and 24) mice (**a**) and young heterochronic parabionts pre and post parabiotic pairing (**b**). **c,d,** Young adult male mice (2-3 months old) were injected with recombinant MCSF or PBS (vehicle) control through intraperitoneal injections four times over ten days. Neurogenesis was analyzed by immunostaining for Dcx. **c,** A representative field of Dcx-positive cells is shown for each treatment group. (scale bar: 100 μm). **d,** Quantification of neurogenesis in the DG after systemic drug administration. Data are from 5 mice per group. Bars show mean + SEM; n.s, not significant; t-test (**b,d**) or ANOVA, Dunnet's post-hoc test (**a**).

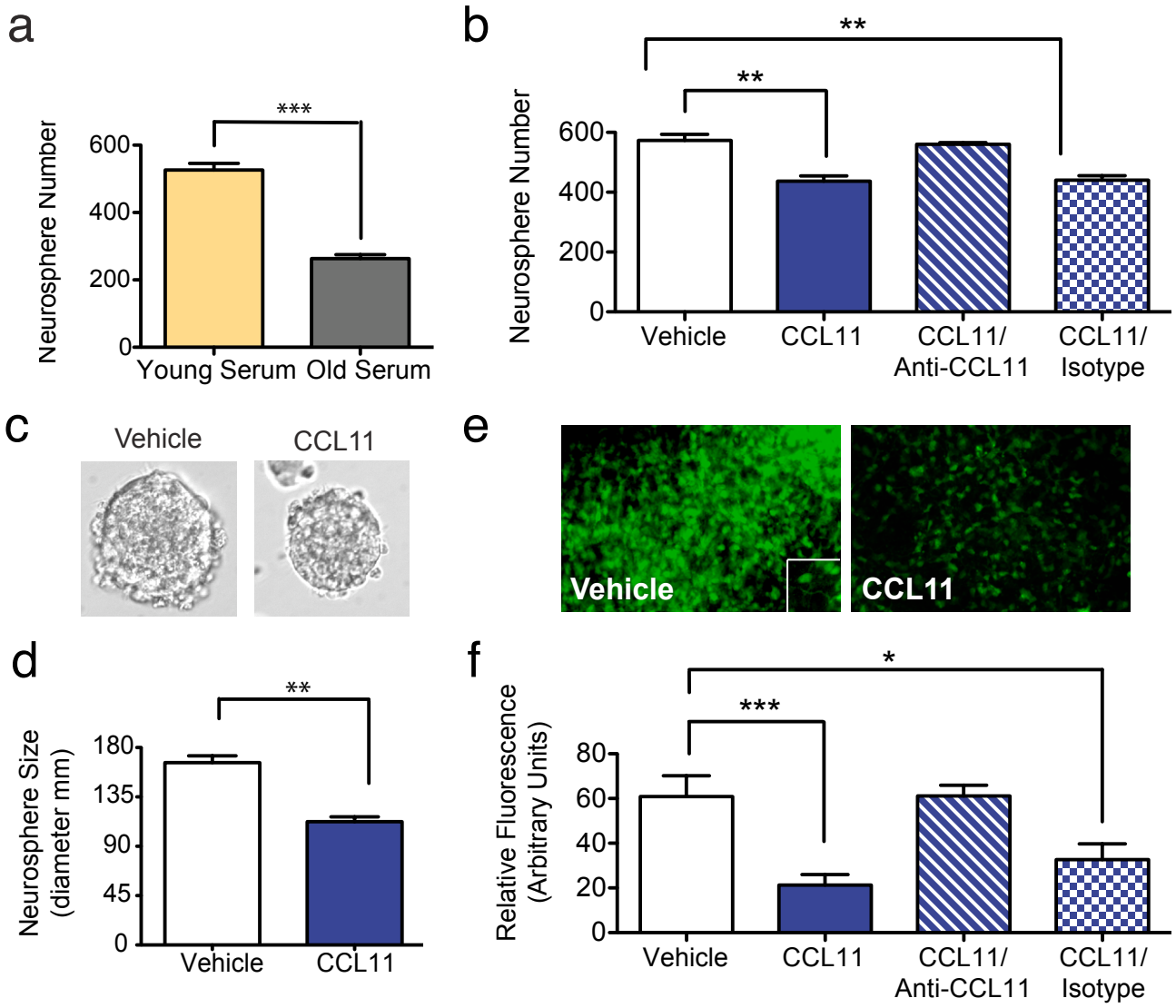

S13. CCL11 inhibits NPC function and neural differentiation in vitro. a, Primary NPCs were exposed to serum isolated from young (2-3 months) or old (18-22 months) mice for four days in culture under self-renewal conditions. The number of neurospheres formed in the presence of old serum was decreased compared to young serum. **b,** Decrease in neurosphere formation after exposure to CCL11 compared with PBS (vehicle) control is rescued by addition of anti-CCL11 neutralizing antibody but not a non-specific isotype control antibody. **c,d,** Representative images (**c**) and quantification (**d**) of decreased neurosphere size after exposure to CCL11. **e,f,** Representative images (**e**) and quantification (**f**) of decreased neuronal differentiation as a function of reduced expression of Dcx promoter-controlled eGFP in stably transfected human derived NTERA cells after exposure to human CCL11 compared with PBS (vehicle) control. **f,** Decreased neuronal differentiation is rescued by addition of anti-CCL11 neutralizing antibody but not by a non-specific isotype control antibody. Dcx reporter gene activity was measured as fluorescence intensity. In vitro data are representative of three independent experiments done in triplicate. Bars are mean + SEM; *P< 0.05; **P< 0.01; ***P< 0.001; t-test (a,d) or ANOVA, Dunnet's post-hoc test (b,d,f).

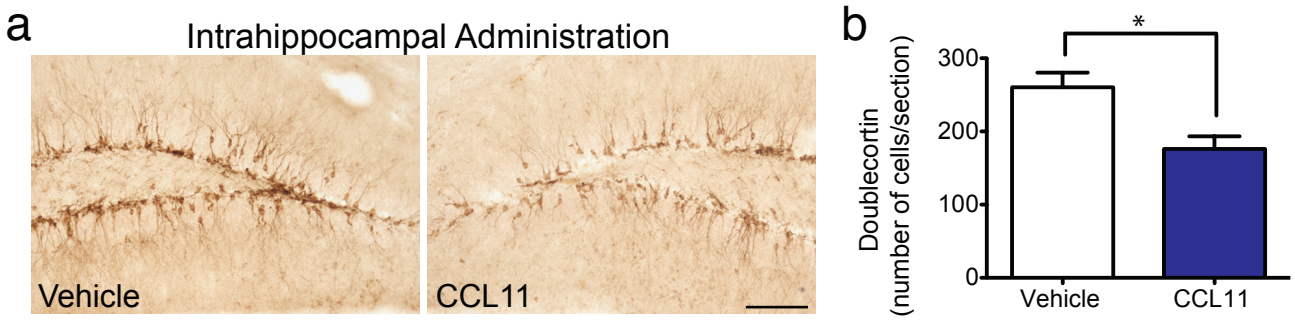

S14. Neurogenesis is inhibited by direct exposure to CCL11 in vivo. Young adult mice were injected stereotaxically with either recombinant CCL11 or PBS into the left or right DG. **a,** A representative field of Dcx-positive cells in adjacent sides of the DG within the same section are shown for treatment groups. **b,** Quantification of neurogenesis in the DG after stereotactic CCL11 administration. Data are from 4-5 young adult mice (2-3 months of age) per group Bars show mean + SEM; *, P< 0.05; t-test.

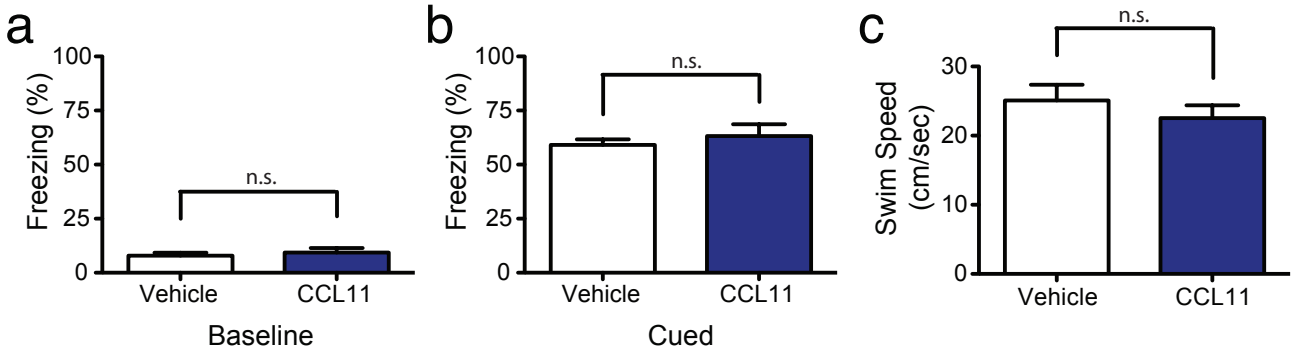

S15. Cued memory and swim speeds are not altered by systemic CCL11 administration. a-c, Normal young (3 months) adult male mice injected intravenously with plasma isolated from young (3-4 months) and old (18-20 months) mice every three days for 24 days. **a,b,** Conditioned fear was displayed as freezing behavior. **a,** Animals intravenously injected with young or old plasma exhibited similar baseline freezing time during training. **b,** No differences in cued memory were detected between groups when re-exposed to the conditioned stimulus (tone and light) in a novel context 24 hours after training. Data are from 8 animals per group. **c,** Swim speeds of mice injected with young or old plasma during the training phase of the RAWM. Data are from 12 animals per group. Bars are mean + SEM; n.s., not significant; t-test.

Supplemental Table 1

Protein Name	Swiss-Prot Accession Number
Apolipoprotein A1	Q00623
β2-Microglobulin	P61769
Calbindin	P12658
CCL2	P10148
CCL7	Q03366
CCL11	P48298
CCL12	Q62401
CD40	P27512
CD40 Ligand	P27548
Clusterin	Q06890
C Reactive Protein	P14847
Cystatin-C	P01035
Epidermal Growth Factor	P07522
Endothelin-1	P22387
Factor VII	P70375
Fibroblast Growth Factor-9	P54130
Fibroblast Growth Factor-basic	Q9CWU6
Fibrinogen	Q8KOE8
Granulocyte Chemotactic Protein-2	P80221
Granulocyte Macrophage-Colony Stimulating	P01587
Growth Hormone	P19795
GST-alpha	P13745
Haptoglobin	Q61646
Interferon-gamma	P01580
Immunoglobulin A	P01878
Interleukin-10	P18893
Interleukin-11	P47873
Interleukin-12p70	P43431
Interleukin-17	Q62386
Interleukin-18	Q14116
Interleukin-1alpha	P01582
Interleukin-1beta	P10749
Interleukin-2	P04351
Interleukin-3	P01586
Interleukin-4	P07750
Interleukin-5	P04401
Interleukin-6	P08505
Interleukin-7	P10168
Insulin	P01325
Inducible Protein-10	P17515
KC/GROalpha	P12850
Leptin	P41160
Leukemia Inhibitory Factor	P09056
Lymphotactin	P47993
Macrophage-Colony Stimulating Factor	P07141
Macrophage-Derived Chemokine	Q54656
Macrophage Inflammatory Protein-1alpha	P10855
Macrophage Inflammatory Protein-1beta	P14097
Macrophage Inflammatory Protein-1gamma	P51670
Macrophage Inflammatory Protein-2	P10889
Macrophage Inflammatory Protein-3beta	2404 (NCBI ID)
Matrix Metalloproteinase-9	P41245
Myoglobin	P04247
NGAL	P11672
Oncostatin M	P08721
Osteopontin	P10923
RANTES	P30882
Stem Cell Factor	P20826
Serum Glutamic-Oxaloacetic Transaminase	P05201
Tissue Inhibitor of Metalloproteinase Type-1	P12032
Tissue Factor	P20352
Tumor Necrosis Factor-alpha	P06804
Thrombopoietin	P40226
Vascular Cell Adhesion Molecule-1	P29533
Vascular Endothelial Cell Growth Factor	Q00731
von Willebrand Factor	Q8C1Z8